



Contents list available at IJRED website

**International Journal of Renewable Energy Development**

Journal homepage: <https://ijred.undip.ac.id>



Research Article

# Grey wolf optimization and incremental conductance based hybrid MPPT technique for solar powered induction motor driven water pump

Divya Shetty<sup>id</sup> and Jayalakshmi Narayana Sabhahit<sup>id\*</sup>

*Department of Electrical and Electronics, Manipal Institute of Technology, Manipal Academy of Higher Education, Manipal 576104, India*

**Abstract.** The use of Solar Powered Water Pumps (SPWP) has emerged as a significant advancement in irrigation systems, offering a viable alternative to electricity and diesel-based pumping methods. The appeal of SPWPs to farmers lies in their low maintenance costs and the incentives provided by government agencies to support sustainable and cost-effective agricultural practices. However, a critical challenge faced by solar photovoltaic (PV) systems is their susceptibility to power loss under partial shading conditions, which can persist for extended periods, ultimately reducing system efficiency. To address this issue, this paper proposes the integration of Maximum Power Point Tracking (MPPT) controllers with efficient algorithms designed to identify the peak power during shading events. In this study, a hybrid approach combining Grey Wolf Optimization (GWO) and Incremental Conductance (INC) is employed to maximize the power output of SPWPs driven by an induction motor under partial shading conditions. In order to achieve faster convergence to the global peak, GWO handles the first stages of MPPT and then INC algorithm is employed at the end of the MPPT process. This method reduces the computations of GWO and streamlines the search space. The paper evaluates the performance of the induction motor in terms of speed settling time and torque ripple. To validate the effectiveness of the GWO-INC hybrid approach, simulations are conducted using the MATLAB Simulink platform. The outcomes are then compared with results obtained from various well-known approaches, including Particle Swarm Optimization – Perturb and Observe (PSO-PO), PSO-INC, and GWO-PO, illustrating the superiority of the GWO-INC hybrid approach in enhancing the efficiency and performance of solar water pumps during shading. The GWO-INC excels with 99.6% accuracy in uniform shading and 99.8% in partial shading. It achieves convergence in a mere 0.55 seconds under uniform shading conditions and only 0.42 seconds when partial shading is present. Moreover, it significantly reduces torque oscillations, with a torque ripple of 8.26% in cases of uniform shading and 10.56% in partial shading.

**Keywords:** solar power, water pump, hybrid MPPT technique, partial shading, motor control.



@ The author(s). Published by CBIORE. This is an open access article under the CC BY-SA license (<http://creativecommons.org/licenses/by-sa/4.0/>).

Received: 5<sup>th</sup> August 2023; Revised: 25<sup>th</sup> Oct 2023; Accepted: 11<sup>th</sup> Nov 2023; Available online: 21<sup>st</sup> Nov 2023

## 1. Introduction

Solar energy has long been a valuable resource for humanity, and with advancements in technology, Solar Photovoltaic (PV) systems play a crucial role in conserving fossil fuels. Solar Powered Water Pumps (SPWP) have emerged as a vital application, particularly in aiding farmers in arid regions where rainfall is scarce. Furthermore, the government is actively encouraging the adoption of solar-based systems and offering subsidies to support their implementation in agricultural operations. Recent developments in SPWP technology have been documented by Aliyu *et al.* (2018). Control strategies for SPWP are extensively reviewed in works by Chandel, Nagaraju Naik, and Chandel (2015), Poompavai and Kowsalya (2019), and Angadi *et al.* (2021). However, PV systems face challenges, particularly in the presence of shading, which can lead to multiple peaks in PV curves, with only one representing the Maximum Power Point (MPP). Various Maximum Power Point Tracking (MPPT) algorithms have been proposed, with Yang *et al.* (2020) reviewing 62 such algorithms, while Mohapatra *et al.* (2017) and Baba, Liu, and Chen (2020) classify MPPT techniques for partial shading scenarios. Ahmad *et al.* (2017)

have offered insightful observations on the impact of partial shading that will help MPPT designers track the peak more quickly.

The MPPT algorithms fall into three categories: conventional, soft computing, and hybrid. Incremental Conductance (INC) and Perturb and Observe (PO) are two extensively used conventional approaches that are simple to apply as discussed by Liu, Meng, and Liu (2016). Both approaches can successfully track peak power if all the panels are exposed to the same amount of sunlight, but they fall short when partial shade occurs. Soft computing-based algorithms pose complexity but are very accurate in detecting the peak power during shaded conditions. Soft computing-based algorithms, particularly those involving Artificial Intelligence, have been compared and evaluated by Yap, Sarimuthu, and Lim (2020) and Rezk *et al.* (2019). Some evolutionary algorithms used in soft computing include Particle Swarm Optimization (PSO) and Grey Wolf Optimization (GWO) which have been elaborated by Seyedmahmoudian *et al.* (2016). GWO technique, in particular, is utilized in scenarios of partial shading by Mohanty, Subudhi, and Ray (2016), where it is compared with

\* Corresponding author  
Email: [jayalakshmi.ns@manipal.edu](mailto:jayalakshmi.ns@manipal.edu) (J.N. Sabhahit)

PO and PSO methods. GWO is found to have better tracking efficiency in comparison with the other two techniques. It also offers lesser oscillations in steady state along with better convergence time. Hybrid technology attempts to combine conventional approaches with soft computing to gain the advantages of each while minimizing their drawbacks. The highlights of the hybrid methods are presented by Bollipo, Mikkili, and Bonthagorla (2021). Hybrid MPPT techniques like PSO-INC and PSO-PO are commonly employed, offering robust performance even in the presence of shading conditions. Sundareswaran, Vignesh Kumar, and Palani (2015) and Abdulkadir and Yatim (2014) present the implementation of PSO-PO and PSO-INC, respectively. GWO is combined with PO to implement MPPT in partial shading scenario by Mohanty, Subudhi, and Ray (2017) where the hybrid method is compared with GWO and PO-PSO methods, and is found to have faster convergence in comparison with the other two techniques.

In SPWP, commonly used motors are Induction Motors (IM), Permanent Magnet Synchronous Motors (PMSM), Brushless DC Motors (BLDC), and Switched Reluctance Motors (SRM). The selection of motors depends on various factors, as reviewed by Narendra *et al.* (2020) and Muralidhar and Rajasekar (2021). A two-stage PMSM-driven SPWP system was optimized using a fuzzy-based PI controller to enhance performance in dynamic and steady-state conditions in the research conducted by Murshid and Singh (2019) with the authors adopting the INC method for MPPT. Antonello *et al.* (2017) have implemented a single stage SPWP driven PMSM utilizing variable step size INC to mitigate the effects of uniform shading. Research by Priyadarshi *et al.* (2022) examines the practical performance evaluation of PV water pump-based PMSM drives where the MPPT is based on a modified firefly algorithm. A grid-connected BLDC solar water pump is proposed with bidirectional power flow by Kumar and Singh (2019) however, it specifically addresses uniform shading conditions. The article by Kashif and Singh (2023) introduces the modified active-power model reference adaptive system to eliminate the current and speed sensors from the solar-based PMSM-driven water pump. The control method that is suggested in the paper by Taibi *et al.* (2023) combines the fuzzy logic mechanism with the traditional P&O algorithm for PMSM-based SPWP. A solar-powered BLDC-driven water pump is proposed with the focus on position sensorless control in the research work of Kumar and Singh (2019) but with no emphasis on shading. A comparison of the hybrid whale optimization-PO method with genetic and evolutionary algorithms is offered for BLDC-based solar water pumps in the literature by Malla *et al.* (2022). An MPPT method has been presented by Ammar *et al.* (2022) for solar water pump driven by BLDC motor to improve the control performance in partial shade situations. The method is based on the cuckoo swarm optimization method. Two MPPT methods - GMPP-based Differential Evolution method and the traditional PO, are used to assess the effects of shading on SRM solar water pumps in the research article by Ibrahim *et al.* (2019). Priyadarshi *et al.* (2020) have presented a SPWP that is SRM-driven and have applied hybrid GSA-PSO MPPT in their research. Khadija *et al.*, (2023) present a solar-powered PV pumping system using a DC-DC boost converter to drive a centrifugal water pump with a BLDC motor, while employing PSO and GWO MPPT methods in partial shading conditions. Priyadarshi *et al.*, (2022) introduce a hybrid GWO-FLC MPPT technique for an SRM-driven PV water pump.

Given their durability, ease of maintenance, and rugged construction, induction motors are a practical choice for agricultural SPWP applications. Periasamy, Jain, and Singh

(2015) have reviewed DC motor and IM-based SPWP. The authors Vitorino *et al.* (2011) have offered control and design improvements for an effective SPWP based on IM. The impact of partial shading on the SPWP driven by IM is examined by Mudlapur *et al.* (2019). A vector-controlled IM-based SPWP is investigated with INC MPPT, however, the effects of shading are not considered in the study conducted by Shukla and Singh (2018). For a smart solar photovoltaic water pumping system, a dynamic reconfiguration method is offered by Gadiraju, Barry, and Jain (2022); nevertheless, the proposed system uses a regular MPPT algorithm to track the maximum power. Arfaoui *et al.* (2019) have reported the research work adopting Salp Swarm Algorithm (SSA) in IM-based SPWP for the MPPT technique.

The effectiveness of PV systems is significantly influenced by partial shading, making the choice of the appropriate MPPT algorithm pivotal. Slow MPPT tracking can delay the motor's attainment of steady-state speed, and high-power oscillations can result in increased motor torque ripples. The existing literature reveals limited exploration of hybrid algorithms for IM-based SPWP. Interestingly, the GWO-INC hybrid algorithm remains uncharted in the context of solar water pump applications. Comparatively, GWO appears to be a more promising choice due to its enhanced accuracy and faster convergence time. Aguila-Leon *et al.*, (2023) present an enhanced MPPT controller for solar systems, using the GWO algorithm, which outperforms traditional methods by increasing output power by 6%, improving efficiency by 3%, and offering faster response times with reduced power fluctuations. Furthermore, within conventional methods, the INC approach consistently delivers superior results, particularly in minimizing steady-state oscillations as is presented in the work by Jayabaskaran *et al.*, (2023).

In light of the preceding discussion, this research work offers several significant contributions. Firstly, it explores the feasibility of employing a hybrid approach that combines GWO and INC to enhance the performance of an IM-based SPWP setup. This approach is compared to other well-established hybrid algorithms like PSO-PO, PSO-INC, and GWO-PO. Secondly, the study evaluates the impact of this chosen hybrid optimization strategy on both the accuracy and convergence time. These assessments are anticipated to lead to potential enhancements in the system's reliability, particularly in achieving a shorter settling time for the motor speed, thereby promoting stable SPWP operation. Lastly, the research delves into an analysis of the potential reduction in steady-state power oscillations achieved through the proposed hybrid approach. It places a specific emphasis on mitigating fluctuations in the DC link voltage, which, in turn, contributes to reducing current and torque ripples in the induction motor.

## 2. Design of IM based solar powered water pump

This section details the configuration of the entire SPWP system. The water pump receives its power from the solar array through a two-stage process. The first stage involves a DC-DC boost converter, and the second stage entails a three-phase inverter. This inverter supplies power to a three-phase Induction Motor (IM) that is connected to a centrifugal pump.

### 2.1 Solar PV Array

The solar array is configured using PV modules arranged in a series-parallel configuration, as depicted in Figure 1(a). When uniform shading occurs, only a single peak is visible in the PV curve. However, PV modules can experience partial shading

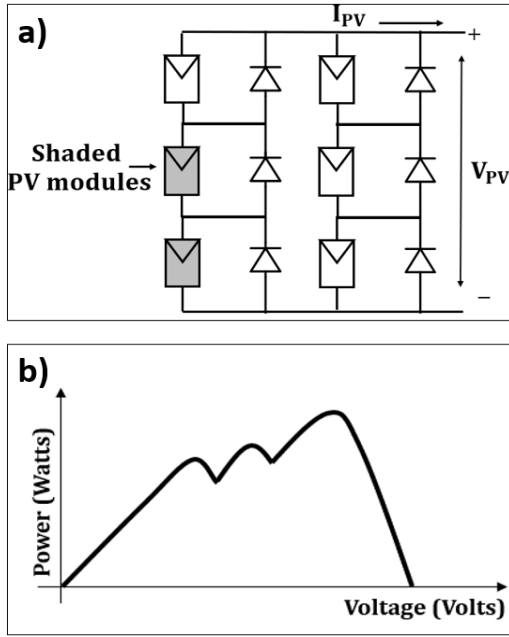


**Fig. 1 a)** Partially Shaded PV array **b)** PV curve of partially shaded PV array

due to factors like clouds, dust, or bird droppings. To mitigate the impact of shading, diodes are connected in parallel across each module. This arrangement leads to the emergence of multiple peaks in the PV curve when shading occurs, as illustrated in Figure 1(b). It is crucial for the Maximum Power Point Tracking (MPPT) system to identify the global peak among all these local peaks.

To simulate the PV system while accounting for shading, a MATLAB Simulink model is developed based on the research conducted by Ding et al. (2012). The expression for Short Circuit (SC) current  $I_{sc}$  is represented as,

$$I_{sc} = I_{SCREF} \times [1 + \alpha(T - T_{REF})] \times \left[ \frac{S}{S_{REF}} \right] \quad (1)$$

where,  $T_{REF}$  is the module's reference temperature when taking Standard Testing Conditions (STC) into account and  $T$  is temperature of PV module. The solar insolation and reference insolation at STC, respectively, are denoted by  $S$  and  $S_{REF}$ . SC current for STC is  $I_{SCREF}$ . The Open Circuit (OC) voltage  $V_{OC}$  is defined as follows,

$$V_{OC} = V_{OCREF} \times n \times \left[ 1 + \alpha \ln \left( \frac{S}{S_{REF}} \right) + \beta(T - T_{REF}) \right] \quad (2)$$

where,  $V_{OCREF}$  is the OC voltage for Standard Testing Conditions. The  $I_{sc}$  and  $V_{OC}$  temperature coefficients are denoted by  $\alpha$  and  $\beta$  respectively.  $I$  is the PV panel current shown as below,

$$I = I_{REF} \times \frac{I_{sc}}{I_{SCREF}} \quad (3)$$

where  $I_{REF}$  is STC current. The PV system specification is shown in Table 1.

### 2.2 DC-DC converter for MPPT controller

In order to efficiently transfer the peak power generated by the PV system to the load, a DC-DC converter is essential. Among the available options, a boost converter, as depicted in Figure 2, is a prudent choice since it demands fewer PV modules.

The converter's design needs to accommodate the variable solar insolation, and the design procedure outlined by Ayop and Tan (2018) serves as a reference. The varying solar insolation causes the PV resistance  $R_{mp}$  to vary from a minimum value  $R_{mp(min)}$  to maximum value of  $R_{mp(max)}$ . The relation between the input resistance  $R_{mp}$  and the output resistance  $R_o$  of the converter is as follows,

$$R_o = \frac{R_{mp}}{(1-D)^2} \quad (4)$$

where load resistance  $R_o$  can range from a minimum value to a maximum value  $R_{o(max)}$ . Rearranging the equation (4), the duty cycle  $D$  applied to the converter is defined as follows,

$$D = 1 - \sqrt{\frac{R_{mp}}{R_o}} \quad (5)$$

The input capacitance  $C_i$  is derived from the change in charge ( $\Delta Q$ ), calculated from the input capacitor's current waveform observed over a specified time interval and is defined as below,

$$C_i = \frac{D}{8L \frac{\Delta V_{mp}}{V_{mp}} f_s^2} \quad (6)$$

where,  $V_{mp}$  is the PV voltage at MPP and serves as the input to the converter.  $\Delta V_{mp}$  is the voltage ripple seen on the PV voltage. The switching frequency is denoted by  $f_s$  and  $L$  is the inductance

**Table 1**  
PV System Specifications

Reference MPP Power	140 W
Voltage at MPP	7 V
Current at MPP	20 A
Open Circuit Voltage	8 V
Short Circuit Current	25 A
Reference Temperature	25 °C
Reference of Solar Insolation	1000 W/m <sup>2</sup>
PV Panels: Total number	10

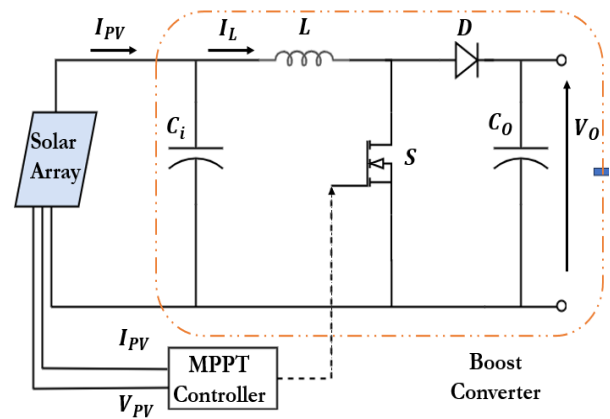


**Fig. 2** Boost Converter Schematic

**Table 2**  
Boost Converter Specifications

Output Power (PO)	4000 W
Input voltage ( $V_{mp}$ )	200 V
Input Capacitor ( $C_i$ )	500 $\mu$ F
Output Voltage ( $V_o$ )	800 V
Ripple in inductor current ( $\Delta i_L$ )	30%
Inductor (L)	10 mH
Output Capacitor ( $C_o$ )	200 $\mu$ F
Ripple in output voltage ( $\Delta V_o$ )	1%

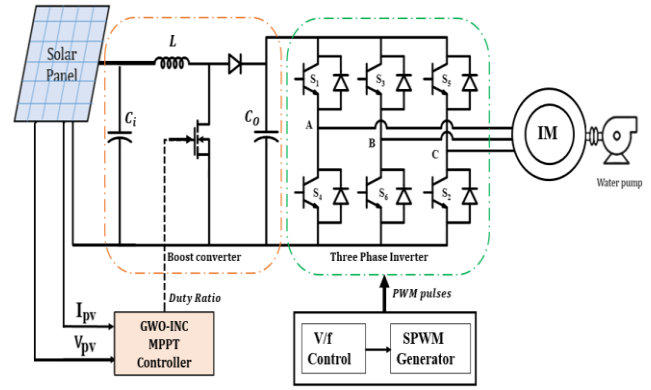


**Fig. 4** Block diagram of SPWP driven by IM.

of the converter. The minimum value of the inductance  $L_{min}$  in the converter depends on the parameters as shown below,

$$L_{min} = \frac{I_L R_{mp(max)}}{\Delta i_L f_s} \left( 1 - \sqrt{\frac{R_{mp(max)}}{R_{O(max)}}} \right) \quad (7)$$

where,  $\Delta i_L$  is the ripple seen on the inductor current and  $I_L$  is the average inductor current.  $C_o$ , the output capacitance is derived from the output capacitor current waveform and is shown below,

$$C_o = \frac{D(1-D)^2}{R_{mp} \frac{\Delta V_o}{V_o} f_s} \quad (8)$$

where,  $\Delta V_o$  is the ripple seen on the output capacitor voltage  $V_o$ . Table 2 displays the specifications of the converter.

### 2.3 Inverter for V/f control of Induction motor

The electromagnetic torque  $T_E$  developed by the three-phase IM can be represented using the dq model as shown below,

$$T_E = \frac{3}{2} \times \frac{Poles}{2} \times [\psi_{DS} \times I_{QS} - \psi_{QS} \times I_{DS}] \quad (9)$$

where  $I_{QS}$  and  $I_{DS}$  are the quadrature and direct axis stator currents respectively. The stator q and d axis flux linkages,  $\psi_{DS}$  and  $\psi_{QS}$  are given by the following representations,

$$\frac{d\psi_{DS}}{dt} = V_{DS} - R_S \times I_{DS} \quad (10)$$

$$\frac{d\psi_{QS}}{dt} = V_{QS} - R_S \times I_{QS} \quad (11)$$

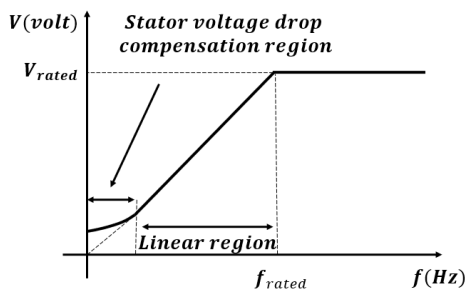


**Fig. 3** Variation of frequency with voltage in V/f control

where  $V_{DS}$  and  $V_{QS}$  are the d and q axis stator voltages.  $R_S$  is the stator resistance. The angular velocity of the rotor  $\omega_r$  is defined as below,

$$\frac{d\omega_r}{dt} = \frac{Poles}{2J} \times (T_E - T_L) \quad (12)$$

where  $T_L$  is the load torque and  $J$  is moment of inertia. In agricultural applications, where cost-effectiveness is paramount, the Voltage-to-Frequency (V/f) control method emerges as the preferred choice for regulating the speed of IMs. This approach involves simultaneous adjustments of both voltage and frequency to maintain a consistent magnetic flux within the motor. The nature of the voltage and frequency in V/f control of IM is shown in Figure 3. The complete system of SPWP is shown in Figure 4. A Sinusoidal Pulse Width Modulation (SPWM) based three phase inverter is used to carry out the V/f control. The SPWM method allows for the precise adjustment of both frequency and output voltage. To counteract the drop across the stator resistance  $R_S$  at zero stator frequency, the motor line-to-line voltage  $V_{LL}$ , must be of finite magnitude, represented by  $V_{OS}$  as defined as,

$$V_{OS} = I_{Sph} R_S \quad (13)$$

where,  $R_S$  is the stator winding resistance and  $I_{sph}$  is the stator current. At low frequencies, the voltage drop  $V_{OS}$  remains constant because it is solely determined by the product of  $R_S$  and  $I_{sph}$ . This constancy results from the fact that the impact of the leakage reactance becomes significant only at higher frequencies. Therefore, it is only within this low-frequency range that the ratio of voltage to frequency ( $V/f$ ) exhibits variation. In the linear region (high-frequency region) the ratio ( $V/f$ ) is constant. As a consequence, the motor line-to-line voltage  $V_{LL}$  will be the sum of stator drop  $V_{OS}$  and  $K_v$  times the frequency  $f$  as shown in the expression below,

$$V_{LL} = V_{OS} + K_v f \quad (14)$$

where  $K_v$  represents the V/f constant and  $f$  is the stator frequency. The line-line voltage  $V_{LL}$  is supplied from a three-phase inverter and is represented as below,

$$V_{LL} = 0.612 m_a V_{DC} \quad (15)$$

where  $m_a$  is the amplitude modulation ratio and  $V_{DC}$  is DC link voltage applied to the inverter. The expression for the constant

**Table 3**  
Specifications of three phase induction motor

Inertia (J)	0.0131 kg-m <sup>2</sup>
Rotor & Stator Self-Inductance (L <sub>R</sub> & L <sub>S</sub> )	0.005839 H
Rotor & Stator Resistance (R <sub>R</sub> & R <sub>S</sub> )	1.395 Ω & 1.405 Ω
Mutual Inductance (L <sub>M</sub> )	0.1722 H
Motor Rating (P)	4000 W
Voltage (V), Rated speed (N <sub>r</sub> )	400 V, 1430 rpm

$K_v$  can be determined under the rated conditions of the motor and is defined below,

$$K_v = \frac{V_{LL} - V_{OS}}{f} \tag{16}$$

Combining equation (14) and equation (15), the expression for  $m_a$  is derived as below,

$$m_a = \frac{V_{OS} + K_v f}{V_{DC} \times 0.612} \tag{17}$$

The line-to-line voltage applied to the motor can be adjusted by varying the frequency since this influences  $m_a$ . Considering a centrifugal pump, the load torque  $T_L$  is represented as below,

$$T_L = K_{pump} \omega_r^2 \tag{18}$$

where  $\omega_r$  and  $K_{pump}$  represent the rotor speed in rad/sec and the pump constant respectively. Specification of three-phase IM is shown in Table 3.

**3. MPPT algorithms**

This section provides an overview of the different Maximum Power Point Tracking (MPPT) algorithms employed for the comparative analysis. The primary emphasis of the study centers on the hybrid approach involving GWO algorithm and the INC algorithm. The section begins by introducing the GWO algorithm and subsequently delves into the hybrid GWO-INC approach.

*3.1 Grey Wolf Optimization Algorithm*

Among the soft computing techniques, Evolutionary algorithms are effective in tracking the global peak under shading conditions. Optimization methods such as PSO and GWO fall under this category. GWO has proven to be more accurate and faster in tracking the optimum point in any scenario. A. Kumar et al., (2022) present an SPV-based water pumping system with a GWO MPPT achieving precise power tracking and minimal computational burden. In GWO, the grey wolves hunt in a pack. There are four groups of wolves but for MPPT application, the number is restricted to three and are named alpha, beta, and gamma. The hunting mechanism of the wolves is modeled by the following expressions,

$$\vec{D} = |\vec{C} \cdot \vec{X}_p(t) - \vec{X}_p(t)| \tag{19}$$

$$\vec{X}(t + 1) = \vec{X}_p(t) - \vec{A} \cdot \vec{D} \tag{20}$$

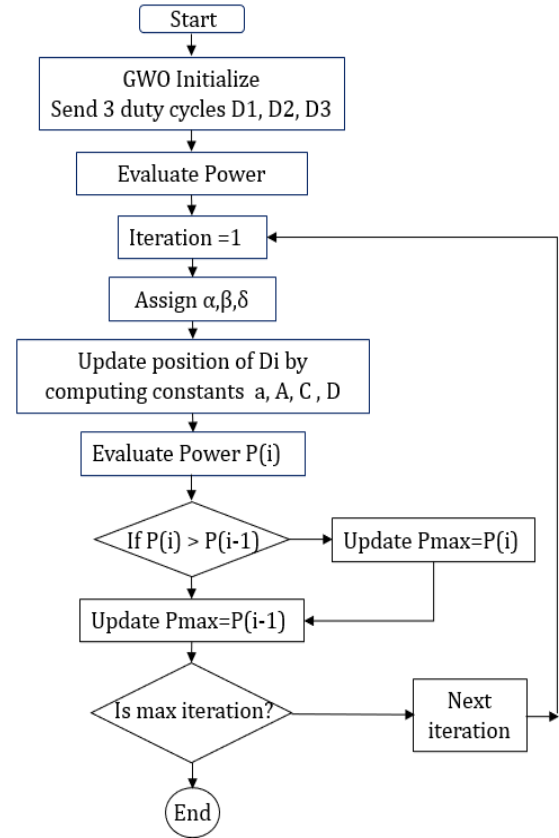


**Fig. 5** Flow chart of GWO

where,  $\vec{X}_p(t)$  is the position vector of the prey and  $\vec{X}$  is the position vector of the grey wolf which in MPPT represents the duty cycle.  $D$  is one of the coefficient vectors. The coefficient vectors,  $A$  and  $C$  are given by the expressions below,

$$\vec{A} = 2\vec{a} \cdot \vec{r}_1 - \vec{a} \tag{21}$$

$$\vec{C} = 2 \cdot \vec{r}_2 \tag{22}$$

where,  $r_1, r_2$  are random vectors. The modified equation to suit the MPPT application is given by the following expression,

$$D_i(k + 1) = D_i(k) - A \cdot D \tag{23}$$

where,  $i$  represents the 3 different wolves: alpha, beta, gamma, and  $k$  is the current iteration. The fitness function is defined as below,

$$P(d_i^k) > P(d_i^{k-1}) \tag{24}$$

where,  $d_i$  is the duty cycle and  $P$  is the photovoltaic power output, which serves as the objective function to be maximized. There are some constraints defined for the MPPT process. The first constraint enforces a cap on the wolf count, set explicitly at three, with the objective of expediting computational speed. The second constraint pertains to the permissible range of duty cycles, as defined as below,

$$0.1 < d_i < 0.9 \tag{25}$$

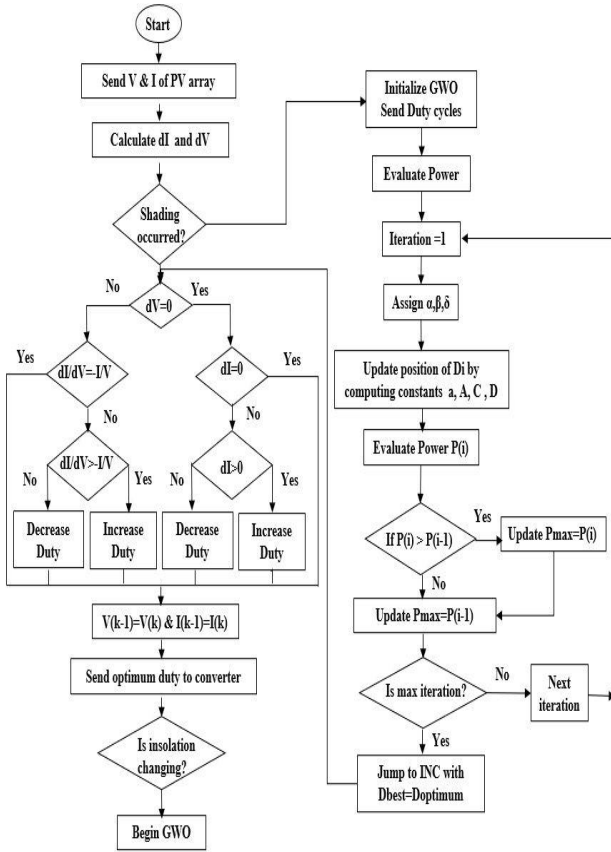


Fig. 6 Flow chart of GWO-INC

The search space for the wolves is contingent on this range of duty cycles outlined in the algorithm. The Flow chart of GWO is presented in figure 5.

3.2 Hybrid MPPT algorithms

Hybrid methods combine either two conventional, two soft computing or both conventional and soft computing techniques as presented in the review by Belhachat & Larbes, (2018). Since it overcomes the drawbacks of both the traditional and soft computing approaches, the hybrid approach, which blends the two, is more effective. The three most common ones are GWO-PO, PSO-PO, and PSO-INC. As both GWO and INC are better than their MPPT counterparts, GWO-INC is adopted in this paper. The flow chart of GWO-INC is shown in Figure 6. Combining GWO and INC, will produce a better result because GWO requires a lot of computations that are unnecessary for uniform shading. When shading is uniform, INC is triggered, and during partial shading, GWO is invoked. The objective function is the PV power output  $P_{PV}$  which is calculated from the PV voltage and current defined as below,

$$P_{PV} = V_{PV} \times I_{PV} \tag{26}$$

where,  $V_{PV}$  is the PV voltage and  $I_{PV}$  is the PV current. If there is decrease of 5% or more in the power output of the solar PV system, it's an indication of the occurrence of partial shading and GWO is initialized to search for the peak power. As GWO approaches the peak, the control is transferred to INC for faster

convergence. The transfer takes place when the position of the wolves (duty cycle) differs by less than 1%. The global peak is then held by INC.

4. Results and Discussion

The IM-based SPWP is investigated using MATLAB Simulink platform. This section presents the results of the simulation work. The study starts off by contrasting optimization techniques. The GWO technique is initially used to gauge the SPWP system's performance, and the results are then contrasted with those obtained using the PSO method. A similar performance analysis is conducted with hybrid methodologies. This involves contrasting the GWO-PO method and PSO-PO, then comparing and contrasting the GWO-INC approach and the PSO-INC strategy in great detail. A concise summary of the comparisons between all six algorithms is formulated to make the best choice. Two separate shading scenarios—uniform and partial shadings—were used to conduct the analysis. The patterns of partial shading are as shown in Figure 7. The MPP for shading-1 is of 2630 W and for shading-2 is 1778 W. The MPP for uniform shading of 1000 W/m<sup>2</sup> is 4000 W. The parameters under consideration for comparison include the following:

- Convergence Time/Speed Settling Time: This parameter represents the duration from when shading is introduced to the moment when the system attains its peak power, allowing the motor to reach a stable speed.
- Accuracy of the MPPT Algorithm: This factor evaluates the precision of the MPPT algorithm in discerning the optimal peak power under different shading conditions. Upon comparison, the objective function, which is the photovoltaic power output  $P_{PV}$  is documented for all the methods, and subsequently, the accuracy of each method is determined.
- Torque Ripple: It gauges the extent of motor torque fluctuations occurring during the steady-state oscillations resulting from the MPPT process.

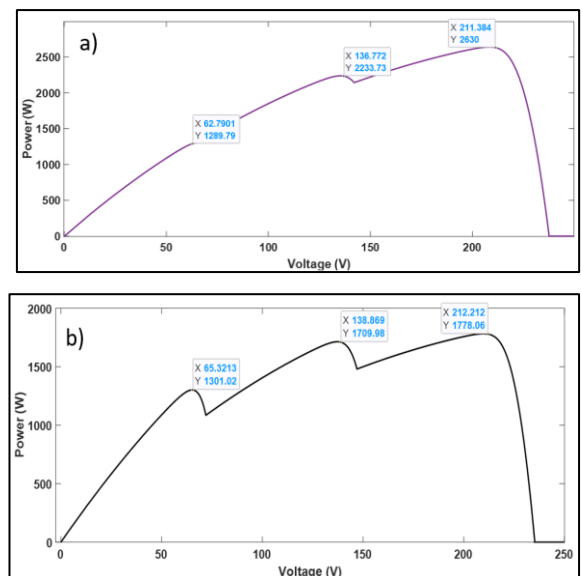


Fig. 7 (a) Partial shading Pattern-1 of PV curve (b) Partial shading Pattern-2 of PV curve

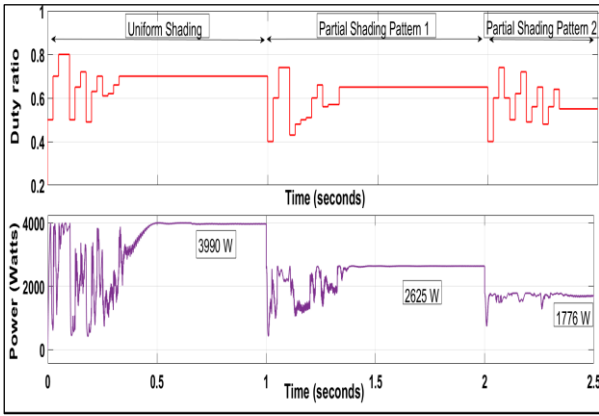


Fig. 8 GWO tracking power for varying shading conditions.

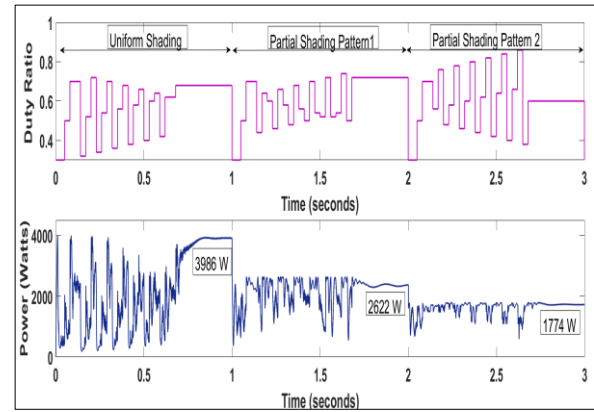


Fig. 10 PSO tracking power for varying shading conditions.

4.1 Comparative Analysis of GWO and PSO

The solar array of the SPWP is placed under uniform shading at the start of simulation. Subsequently, at 1 second into the simulation, partial shading-1 was introduced, followed by the introduction of partial shading-2 at the 2-second mark. To optimize performance under these varying shading scenarios, the GWO technique was applied. Figure 8 illustrates the duty cycle and power output of the solar array under different shading conditions. GWO yielded a duty cycle of 0.71, resulting in a peak power transfer of 3990 W. Similarly, for partial shading-1 and -2, duty cycles of 0.65 and 0.56 were applied, resulting in power outputs of 2625 W and 1776 W, respectively. Figure 9 depicts the changes in motor speed and torque. Under uniform shading, the motor operated close to its rated speed, while for partial shading- 1 and -2, the speed was maintained at 1200 rpm and 1100 rpm respectively. A comparative analysis was conducted with the PSO method, as seen in Figure 10, showcasing the variations in duty with output power. The time required to identify the optimized duty cycle for the GWO approach is 0.45 seconds. In contrast, the PSO algorithm takes 0.8 seconds under uniform shading conditions and 0.85 seconds under partial shading conditions to determine the appropriate duty cycle for optimal power output. The PSO-based power retrieval results are as follows: 3986 W under uniform shading, 2622 W under shading condition 1, and 1774 W under shading condition 2. Notably, these values are lower than the power obtained through GWO. Additionally, Figure 11 visually depicts

Table 4

Performance of GWO and PSO for different shading

MPPT	Performance parameter	Shading Patterns		
		Uniform Shading	Partial Shading 1	Partial Shading 2
GWO	Power ( $P_{PV}$ )	3990 W	2625 W	1776 W
	Convergence Time	0.45 sec	0.45 sec	0.45 sec
	Motor speed	1430 rpm	1200 rpm	1100 rpm
	Torque ripple	0.92%	1.2%	3.76%
PSO	Power ( $P_{PV}$ )	3986 W	2622 W	1774 W
	Convergence Time	0.8 sec	0.85 sec	0.85 sec
	Motor speed	1430 rpm	1170 rpm	1000 rpm
	Torque ripple	1.33%	2.36%	4.2%

the changes in motor speed and torque when employing PSO method. Since PSO retrieves less power compared to GWO, it operates the motor at lower speeds of 1170 rpm and 1000 rpm for partial shading 1 and 2, respectively. These results are also summarized in Table 4, highlighting that GWO excels in tracking the peak more swiftly than PSO, boasting better convergence time and enhanced accuracy for both uniform and partial shading conditions. Furthermore, motor torque ripple was notably lower in the GWO approach compared to PSO. Observations from Table 4. indicate that the GWO method

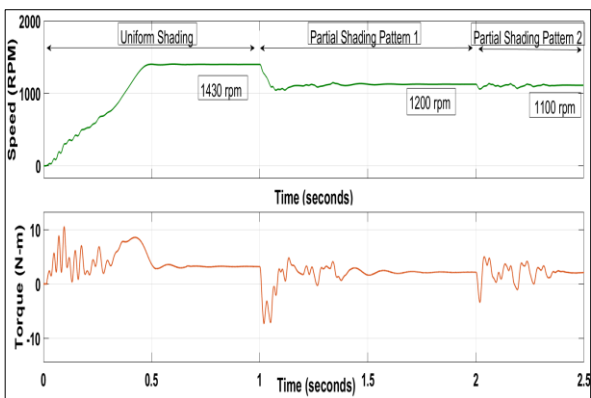


Fig. 9 Speed and torque of IM for varying shading conditions with GWO

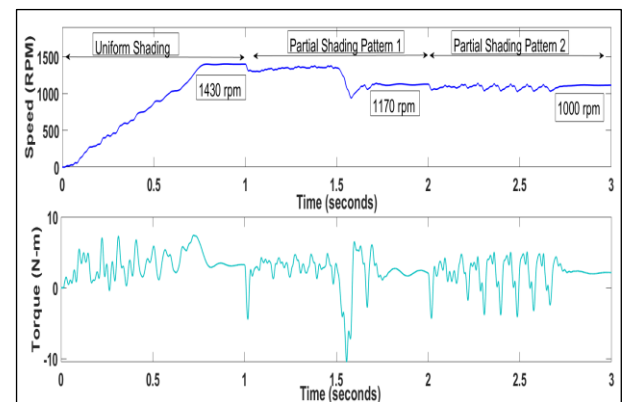
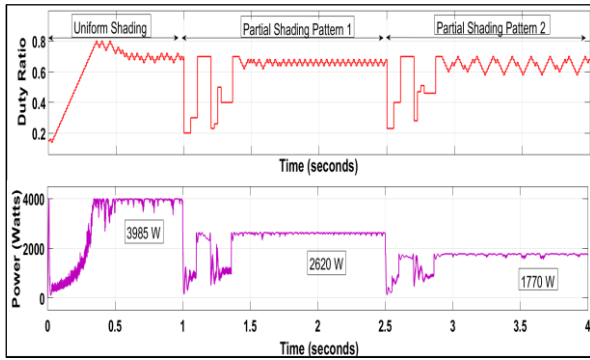
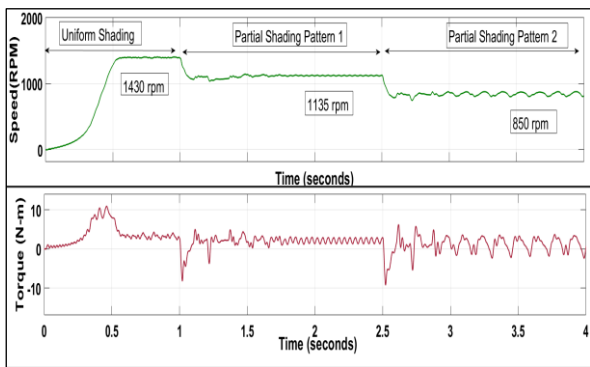


Fig. 11 Speed and torque of IM for varying shading conditions with PSO.



**Fig 12** GWO-PO method tracking power for varying shading conditions



**Fig. 13** Speed and torque of IM for varying shading conditions with GWO-PO

provides a reduction in torque ripple ranging from 0.45% to 1%, encompassing both uniform and partial shading conditions.

#### 4.2 Comparative Analysis of GWO-PO and PSO-PO

The hybrid GWO-PO simulation was employed to assess the performance of the IM-based SPWP. In this setup, the PO method was employed during uniform shading, while GWO took over during partial shading conditions. As GWO approached the peak power, control was handed over to PO to expedite convergence, with the transition occurring when the wolves' positions differed by less than 1%. Subsequently, the global peak was maintained by the PO method.

The SPWP system was initially subjected to uniform shading, followed by the introduction of shading-1 at 1 second and shading-2 at 2.5 seconds. Figure 12 illustrates the solar array output under the various shading patterns, showing convergence of duty cycle in pursuit of the relevant peak power by GWO-PO. Figure 13 presents changes in motor torque and speed under various shading scenarios. During uniform shading, PO managed to capture the power, although its accuracy was not as high as GWO. On the other hand, during partial shading, GWO took the lead in power tracking, resulting in improved accuracy.

Furthermore, a comparative analysis was conducted with the performance of the PSO-PO approach. Figure 14 displays the duty cycle applied to the boost converter and the corresponding peak power for the PSO method, while Figure 15 provides insights into motor speed and torque variations under diverse shading conditions for PSO-PO. The results of both GWO-PO and PSO-PO are comprehensively tabulated in Table 5. In scenarios with uniform shading, GWO-PO, and PSO-PO both demonstrate comparable accuracy in tracking peak power

**Table 5**  
Performance of GWO-PO and PSO-PO for different shading

MPPT	Performance parameter	Shading Patterns		
		Uniform Shading	Partial Shading 1	Partial Shading 2
GWO-PO	Power ( $P_{PV}$ )	3985 W	2620 W	1770 W
	Convergence Time	0.7 sec	0.45 sec	0.45 sec
	Motor speed	1430 rpm	1135 rpm	850 rpm
	Torque ripple	15.76%	17.71%	22.34%
PSO-PO	Power ( $P_{PV}$ )	3985 W	2605 W	1765 W
	Convergence Time	0.7 sec	0.6 sec	0.55 sec
	Motor speed	1430 rpm	1123 rpm	842 rpm
	Torque ripple	17.34%	18.21%	23.21%

of 3985 W, with a convergence time of 0.7 seconds. This similarity arises from the activation of the PO algorithm in both hybrid methods during uniform shading.

However, when faced with partial shading, GWO-PO outperforms PSO-PO by tracking the peak power levels of 2620 W for shading 1 and 1770 W for shading 2 in just 0.45 seconds.

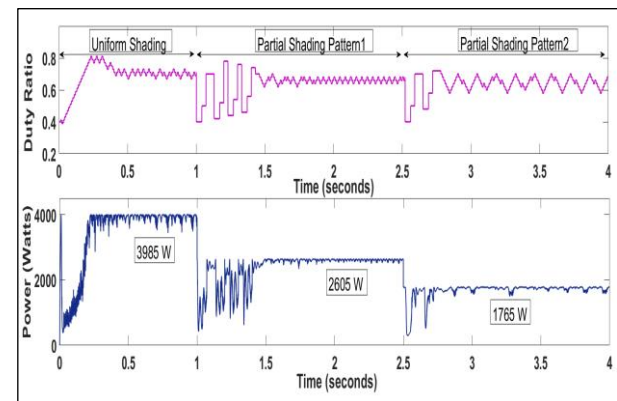


**Fig. 14** PSO-PO process tracking power for varying shading conditions.

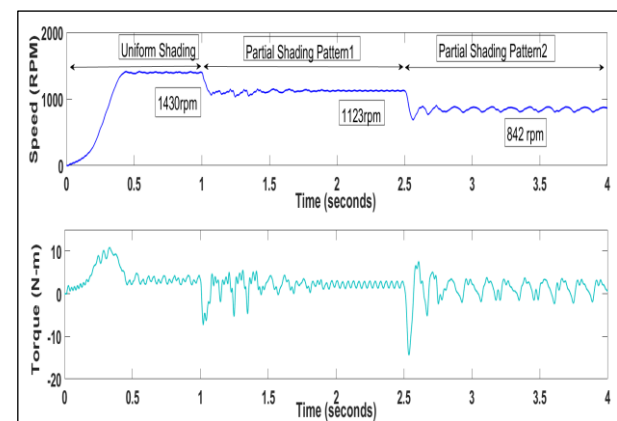


**Fig. 15** Speed and torque of IM for varying shading conditions with PSO-PO

This results in motor speeds of 1135 rpm and 850 rpm for shading 1 and 2, respectively as shown in Figure 13. Table 5 displays that GWO outperforms PSO with an approximately 0.576% increase in tracked power for Shading 1 and 0.283% for Shading 2. Furthermore, Table 5 illustrates that GWO-PO demonstrates an approximately 9.13% improvement over PSO-PO in reducing torque ripple under uniform shading, 2.75% in shading 1, and 3.74% in shading 2. In Table 5, it is evident that GWO-PO exhibits superior accuracy and achieves faster convergence times with reduced torque ripples when compared to PSO-PO. In summary, GWO-PO stands out as the superior choice in both settling time and accuracy in comparison to PSO-PO.

4.3 Comparative Analysis of GWO-INC and PSO-INC

This paper focuses on investigating the hybrid GWO-INC technique. Initially, the SPWP undergoes uniform shading, followed by shading-1 at 1 second and shading-2 at 2.5 seconds. Figure 16 displays the power variation and duty ratio concerning various shading scenarios in the GWO-INC approach. In the presence of uniform shading, the INC method determines the peak power, resulting in an output of 3985 watts. For the two partial shading patterns, the GWO method is employed, resulting in MPP power values of 2625 W for shading-1 and 1772 W for shading-2. Figure 17 illustrates the variation in motor speed and torque. Under uniform shading, the water pump's running speed is 1430 rpm, while it drops to 1175 rpm and 860 rpm under shading-1 and shading-2, respectively.

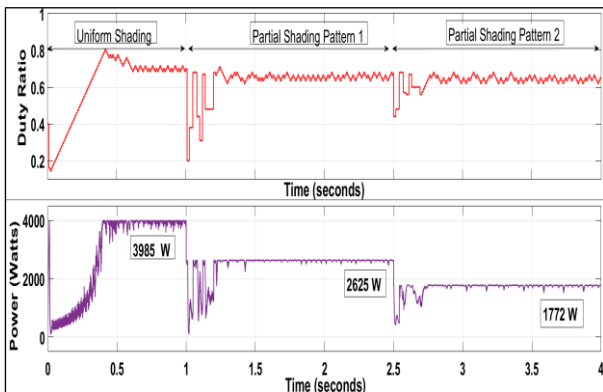


Fig. 16 GWO-INC method tracking power for varying shading conditions.

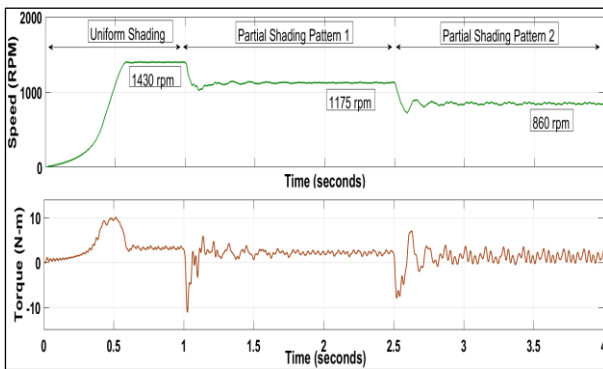


Fig. 17 Speed and torque of IM for varying shading conditions with GWO-INC

Table 6 Performance of GWO-INC and PSO-INC in different shading

MPPT	Performance parameter	Shading Patterns		
		Uniform Shading	Partial Shading 1	Partial Shading 2
GWO-INC	Power ( $P_{PV}$ )	3985 W	2625 W	1772 W
	Convergence Time	0.55 sec	0.42 sec	0.42 sec
	Motor speed	1430 rpm	1175 rpm	860 rpm
	Torque ripple	8.26%	10.56%	15.12%
PSO-INC	Power ( $P_{PV}$ )	3985 W	2618 W	1768 W
	Convergence Time	0.55 sec	0.85 sec	0.85 sec
	Motor speed	1430 rpm	1140rpm	847 rpm
	Torque ripple	10.79%	12.52%	18.21%

These results are compared with the PSO-INC method. Figure 18 shows how duty changes with peak power variation under different shading conditions when employing the PSO-INC method. Figure 19 displays speed and torque ripple values for varying shading scenarios with the PSO-INC technique. A summary of the comparative analysis results is presented in Table 6.

For uniform shading, both hybrid methods converge in the same amount of time (0.55 sec) since INC is utilized in both for uniform shading, tracking a peak power of 3985 W. Notably, the GWO-INC approach exhibits faster settling time under partial shading conditions, with a time of 0.42 seconds, whereas PSO-INC requires 0.85 seconds for partial shading scenarios. This swifter settling time with GWO-INC reduces the likelihood of oscillations or overshooting the target speed, contributing to a more stable operation and minimizing unnecessary wear and tear on mechanical components. Moreover, rapid settling times translate to energy savings, as the motor spends less time accelerating and decelerating.

Both hybrid methods demonstrate similar peak power accuracy when uniform shading is considered, owing to the application of INC. Nonetheless, in scenarios involving partial shading, GWO-INC surpasses the performance of PSO-INC. PSO-INC yields peak power values of 2618 W and 1768 W, whereas the utilization of the GWO-INC method results in MPP power values of 2625 W for shading-1 and 1772 W for shading-2, closely aligning with the actual peak values depicted in Figure

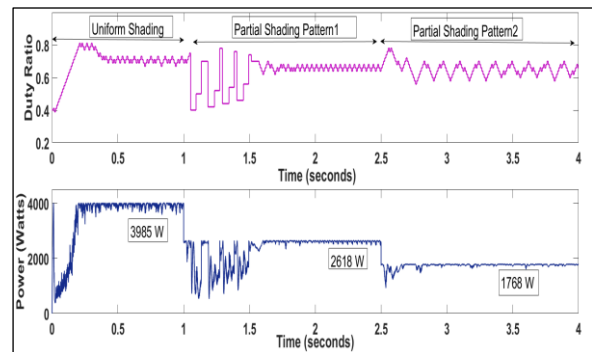
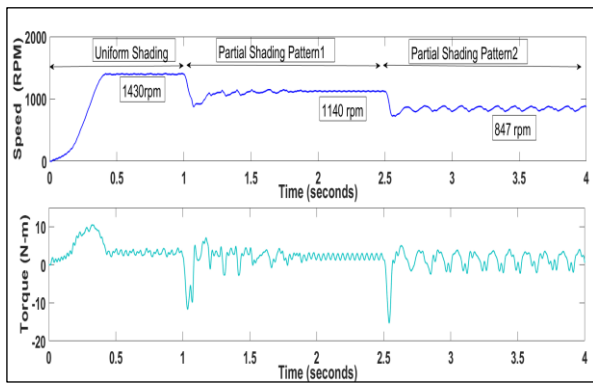


Fig. 18 PSO-INC method tracking power for varying shading conditions.



**Fig. 19** Speed and torque of IM for varying shading conditions with PSO-INC

7. Consequently, the GWO-INC method facilitates higher motor speeds, effectively harnessing PV power and enhancing system efficiency. Table 6 illustrates that GWO-INC outperforms PSO-INC with an approximately 23.48% reduction in torque ripple under uniform shading, 15.65% less ripple in shading 1, and 16.95% reduced ripple in shading 2. Thus, the GWO-INC method exhibits less torque variation than PSO-INC, resulting in more stable and efficient system operation, ultimately reducing long-term maintenance and repair costs.

**4.4 Comparative Analysis of all the six Algorithms**

Table 7 provides a comprehensive assessment of six different algorithms, encompassing optimization methods like GWO, PSO and hybrid approaches like GWO-PO, PSO-PO, GWO-INC, and PSO-INC. The table offers a concise overview of performance metrics, specifically motor torque ripples, speed convergence time, and accuracy, evaluated in both uniform and shaded conditions.

In this comparative evaluation, the GWO-INC approach stands out as the preferred option, given its remarkable precision of 99.6% in uniform shading and 99.8% in partial shading, the swiftest convergence times at 0.55 sec in uniform shading and 0.42 sec in partial shading, as well as a notable reduction in torque oscillations of 8.26% in uniform shading and 10.56% in partial shading. These attributes play a pivotal role in enhancing pump efficiency, curbing energy consumption, and minimizing operational expenses. Additionally, the rapid convergence times and minimal torque fluctuations foster stable pump operation, mitigating the risk of vibrations and augmenting long-term reliability. Ultimately, these advantages alleviate mechanical stress on the pump, leading to an extended lifespan and decreased maintenance and repair costs.

**5. Conclusion**

By harnessing the cost-effective and robust nature of the IM alongside economical V/f control, the SPWP in this work, proves to be a highly effective solution for meeting agricultural irrigation requirements. Furthermore, the GWO-INC technique plays a crucial role in accurately tracking peak power under various shading conditions. To ascertain the method's effectiveness, a comparative analysis is conducted, pitting this hybrid approach against GWO, PSO, GWO-PO, PSO-PO, and PSO-INC. While the GWO offers exceptional precision, it is important to note that in scenarios with uniform shading, high

**Table 7**  
Comparison Of Performance Parameters

	MPPT	Shading	PV power (W)	Settling time of Speed(sec)	Torque ripple	Accuracy
GWO		Uniform	3990	0.45	0.92%	99.75%
		Partial	2625	0.45	1.2%	99.80%
PSO		Uniform	3986	0.8	1.33%	99.65%
		Partial	2622	0.85	2.36%	99.71%
Hybrid GWO-PO		Uniform	3985	0.7	15.76%	99.51%
		Partial	2620	0.45	17.71%	99.54%
Hybrid PSO-PO		Uniform	3985	0.7	17.34%	99.50%
		Partial	2605	0.6	18.21%	99.04%
Hybrid GWO-INC		Uniform	3985	0.55	8.26%	99.60%
		Partial	2625	0.42	10.56%	99.80%
Hybrid PSO-INC		Uniform	3985	0.55	10.79%	99.60%
		Partial	2618	0.85	12.52%	99.54%

processing complexity is unnecessary. In these cases, the INC method efficiently tracks peak power, reducing computational complexity during uniform shading. Comparing INC MPPT to the PO method highlights INC's benefits, including fewer steady-state oscillations, reduced motor current and torque ripples, enhancing system stability and efficiency. Additionally, GWO exhibits rapid convergence compared to PSO, shortening system response time and ensuring steady-state motor speed, contributing to SPWP system stability. Collectively, the GWO-INC approach emerges as superior to other techniques, offering the potential to mitigate power loss during typical instances of partial shading encountered in SPWP installations in agricultural areas. This research contributes to the advancement of sustainable irrigation systems and highlights the potential for optimizing SPWPs in the presence of partial shading conditions.

**Author Contributions:** D.S.: Conceptualization, methodology, software, validation, formal analysis, investigation, resources, writing-original draft, J.N.S.: Visualization, validation, supervision, project administration, review and editing. All authors have read and agreed to the published version of the manuscript.

**Funding:** All authors declare that no funds, grants, or other support were received during the preparation of this manuscript.

**Conflicts of Interest:** The authors declare no conflict of interest.

**References**

Abdulkadir, M., & Yatim, A. H. M. (2014). Hybrid maximum power point tracking technique based on PSO and incremental conductance. *2014 IEEE Conference on Energy Conversion, CENCON 2014*, 271–276. <https://doi.org/10.1109/CENCON.2014.6967514>

Aguila-Leon, J., Vargas-Salgado, C., Chiñas-Palacios, C., & Diaz-Bello, D. (2023). Solar photovoltaic Maximum Power Point Tracking controller optimization using Grey Wolf Optimizer: A performance comparison between bio-inspired and traditional algorithms. *Expert Systems with Applications*, 211(August 2022).

- <https://doi.org/10.1016/j.eswa.2022.118700>
- Ahmad, R., Murtaza, A. F., Ahmed Sher, H., Tabrez Shami, U., & Olalekan, S. (2017). An analytical approach to study partial shading effects on PV array supported by literature. *Renewable and Sustainable Energy Reviews*, 74(December 2016), 721–732. <https://doi.org/10.1016/j.rser.2017.02.078>
- Aliyu, M., Hassan, G., Said, S. A., Siddiqui, M. U., Alawami, A. T., & Elamin, I. M. (2018). A review of solar-powered water pumping systems. *Renewable and Sustainable Energy Reviews*, 87(February), 61–76. <https://doi.org/10.1016/j.rser.2018.02.010>
- Ammar, A., Hamraoui, K., Belguellaoui, M., & Kheldoun, A. (2022). *Performance Enhancement of Photovoltaic Water Pumping System Based on BLDC Motor under Partial Shading Condition*. 22. <https://doi.org/10.3390/engproc2022014022>
- Angadi, S. (2021). Comprehensive Review on Solar, Wind and Hybrid Wind-PV Water Pumping Systems-An Electrical Engineering Perspective. *CPSS Transactions on Power Electronics and Applications*, 6(1), 1–19. <https://doi.org/10.24295/cpsstpea.2021.00001>
- Antonello, R., Costabeber, Alessandro, C., Tinazzi, F., & Zigliotto, M. (2017). Energy-Efficient Autonomous Solar Synchronous Motors. *IEEE Transactions on Industrial Electronics*, 64(1), 43–51.
- Arfaoui, J., Rezk, H., Al-Dhaifallah, M., Elyes, F., & Abdelkader, M. (2019). Numerical performance evaluation of solar photovoltaic water pumping system under partial shading condition using modern optimization. *Mathematics*, 7(11). <https://doi.org/10.3390/math7111123>
- Ayop, R., & Tan, C. W. (2018). Design of boost converter based on maximum power point resistance for photovoltaic applications. *Solar Energy*, 160(August 2017), 322–335. <https://doi.org/10.1016/j.solener.2017.12.016>
- Baba, A. O., Liu, G., & Chen, X. (2020). Classification and Evaluation Review of Maximum Power Point Tracking Methods. *Sustainable Futures*, 2(February). <https://doi.org/10.1016/j.sfr.2020.100020>
- Belhachat, F., & Larbes, C. (2018). A review of global maximum power point tracking techniques of photovoltaic system under partial shading conditions. *Renewable and Sustainable Energy Reviews*, 92(January), 513–553. <https://doi.org/10.1016/j.rser.2018.04.094>
- Bollipo, R. B., Mikkili, S., & Bonthagorla, P. K. (2021). Hybrid, optimal, intelligent and classical PV MPPT techniques: A review. *CSEE Journal of Power and Energy Systems*, 7(1), 9–33. <https://doi.org/10.17775/CSEEJPES.2019.02720>
- Chandel, S. S., Nagaraju Naik, M., & Chandel, R. (2015). Review of solar photovoltaic water pumping system technology for irrigation and community drinking water supplies. *Renewable and Sustainable Energy Reviews*, 49, 1084–1099. <https://doi.org/10.1016/j.rser.2015.04.083>
- Ding, K., Bian, X., Liu, H., & Peng, T. (2012). A MATLAB-simulink-based PV module model and its application under conditions of nonuniform irradiance. *IEEE Transactions on Energy Conversion*, 27(4), 864–872. <https://doi.org/10.1109/TEC.2012.2216529>
- Gadiraju, H. K. V. (2022). Improved Performance of PV Water Pumping System Using Dynamic Reconfiguration Algorithm Under Partial Shading Conditions. *CPSS Transactions on Power Electronics and Applications*, 7(2), 206–215. <https://doi.org/10.24295/cpsstpea.2022.00019>
- Ibrahim, M. N., Rezk, H., Al-Dhaifallah, M., & Sergeant, P. (2019). Solar Array Fed Synchronous Reluctance Motor Driven Water Pump: An Improved Performance under Partial Shading Conditions. *IEEE Access*, 7, 77100–77115. <https://doi.org/10.1109/ACCESS.2019.2922358>
- Jayabaskaran, G., Suresh, S., Gopinath, B., & Geetha, M. (2023). Solar PV Combined Efficient Torque Control of BLDC Motor Using Salp Swarm Optimization. *Electric Power Components and Systems*, 51(13), 1338–1354. <https://doi.org/10.1080/15325008.2023.2196679>
- Kashif, M., & Singh, B. (2023). Modified Active-Power MRAS Based Adaptive Control With Reduced Sensors for PMSM Operated Solar Water Pump. *IEEE Transactions on Energy Conversion*, 38(1), 38–52. <https://doi.org/10.1109/TEC.2022.3197564>
- Khadija, S., Ouadia, E. M., & Abdelmajid, F. (2023). *Tracking the GMPP of a solar photovoltaic water pumping system with an SMC controller in partial shading conditions*. 12(6), 3298–3310. <https://doi.org/10.11591/eei.v12i6.5504>
- Kumar, A., Bilal, M., Rizwan, M., & Nangia, U. (2022). Grey Wolf Optimization Inspired Maximum Power Extraction from SPV System for Water Pumping Application. *2022 International Conference for Advancement in Technology, ICONAT 2022*, 1–6. <https://doi.org/10.1109/ICONAT53423.2022.9726028>
- Kumar, R., & Singh, B. (2019a). Grid Interactive Solar PV-Based Water Pumping Using BLDC Motor Drive. *IEEE Transactions on Industry Applications*, 55(5), 5153–5165. <https://doi.org/10.1109/TIA.2019.2928286>
- Kumar, R., & Singh, B. (2019b). Solar PV powered-sensorless BLDC motor driven water pump. *IET Renewable Power Generation*, 13(3), 389–398. <https://doi.org/10.1049/iet-rpg.2018.5717>
- Liu, L., Meng, X., & Liu, C. (2016). A review of maximum power point tracking methods of PV power system at uniform and partial shading. *Renewable and Sustainable Energy Reviews*, 53, 1500–1507. <https://doi.org/10.1016/j.rser.2015.09.065>
- Malla, S. G., Malla, P., Malla, J. M. R., Singla, R., Choudekar, P., Koilada, R., & Sahu, M. K. (2022). Whale Optimization Algorithm for PV Based Water Pumping System Driven by BLDC Motor Using Sliding Mode Controller. *IEEE Journal of Emerging and Selected Topics in Power Electronics*, 10(4), 4832–4844. <https://doi.org/10.1109/JESTPE.2022.3150008>
- Mohanty, S., Subudhi, B., & Ray, P. K. (2016). A new MPPT design using grey Wolf optimization technique for photovoltaic system under partial shading conditions. *IEEE Transactions on Sustainable Energy*, 7(1), 181–188. <https://doi.org/10.1109/TSSTE.2015.2482120>
- Mohanty, S., Subudhi, B., & Ray, P. K. (2017). A Grey Wolf-Assisted Perturb & Observe MPPT Algorithm for a PV System. *IEEE Transactions on Energy Conversion*, 32(1), 340–347. <https://doi.org/10.1109/TEC.2016.2633722>
- Mohapatra, A., Nayak, B., Das, P., & Mohanty, K. B. (2017). A review on MPPT techniques of PV system under partial shading condition. *Renewable and Sustainable Energy Reviews*, 80(December 2016), 854–867. <https://doi.org/10.1016/j.rser.2017.05.083>
- Mudlapur, A., Ramana, V. V., Damodaran, R. V., Balasubramanian, V., & Mishra, S. (2019). Effect of Partial Shading on PV Fed Induction Motor Water Pumping Systems. *IEEE Transactions on Energy Conversion*, 34(1), 530–539. <https://doi.org/10.1109/TEC.2018.2876132>
- Muralidhar, K., & Rajasekar, N. (2021). A review of various components of solar water-pumping system: Configuration, characteristics, and performance. *International Transactions on Electrical Systems*, 31(9), 1–33. <https://doi.org/10.1002/2050-7038.13002>
- Murshid, S., & Singh, B. (2019). Implementation of PMSM Drive for a Solar Water Pumping System. *IEEE Transactions on Industry Applications*, 55(5), 4956–4964. <https://doi.org/10.1109/TIA.2019.2924401>
- Narendra, A., Venkataramana Naik, N., Panda, A. K., & Tiwary, N. (2020). A Comprehensive Review of PV Driven Electrical Motors. *Solar Energy*, 195(August 2019), 278–303. <https://doi.org/10.1016/j.solener.2019.09.078>
- Periasamy, P., Jain, N. K., & Singh, I. P. (2015). A review on development of photovoltaic water pumping system. *Renewable and Sustainable Energy Reviews*, 43, 918–925. <https://doi.org/10.1016/j.rser.2014.11.019>
- Poompavai, T., & Kowsalya, M. (2019). Control and energy management strategies applied for solar photovoltaic and wind energy fed water pumping system: A review. *Renewable and Sustainable Energy Reviews*, 107(February), 108–122. <https://doi.org/10.1016/j.rser.2019.02.023>
- Priyadarshi, N., Bhaskar, M. S., Padmanaban, S., Blaabjerg, F., & Azam, F. (2020). New CUK-SEPIC converter based photovoltaic power system with hybrid GSA-PSO algorithm employing MPPT for water pumping applications. *IET Power Electronics*, 13(13), 2824–2830. <https://doi.org/10.1049/iet-pel.2019.1154>
- Priyadarshi, N., Maroti, P. K., & Hussien, M. G. (2022). Extensive performance investigation of Luo converter-based modified firefly maximum point tracking algorithm for permanent magnet synchronous motor-driven photovoltaic pumping system. *IET Renewable Power Generation*. <https://doi.org/10.1049/rpg2.12520>
- Priyadarshi, N., Padmanaban, S., Bhaskar, M. S., Azam, F., Khan, B., &

- Hussien, M. G. (2022). A novel hybrid grey wolf optimized fuzzy logic control based photovoltaic water pumping system. *IET Renewable Power Generation*. <https://doi.org/10.1049/rpg2.12638>
- Rezk, H., AL-Oran, M., Gomaa, M. R., Tolba, M. A., Fathy, A., Abdelkareem, M. A., Olabi, A. G., & El-Sayed, A. H. M. (2019). A novel statistical performance evaluation of most modern optimization-based global MPPT techniques for partially shaded PV system. *Renewable and Sustainable Energy Reviews*, 115(August), 109372. <https://doi.org/10.1016/j.rser.2019.109372>
- Seyedmahmoudian, M., Horan, B., Soon, T. K., Rahmani, R., Than Oo, A. M., Mekhilef, S., & Stojcevski, A. (2016). State of the art artificial intelligence-based MPPT techniques for mitigating partial shading effects on PV systems – A review. *Renewable and Sustainable Energy Reviews*, 64, 435–455. <https://doi.org/10.1016/j.rser.2016.06.053>
- Shukla, S., & Singh, B. (2018). Single-Stage PV Array Fed Speed Sensorless Vector Control of Induction Motor Drive for Water Pumping. *IEEE Transactions on Industry Applications*, 54(4), 3575–3585. <https://doi.org/10.1109/TIA.2018.2810263>
- Sundareswaran, K., Vignesh kumar, V., & Palani, S. (2015). Application of a combined particle swarm optimization and perturb and observe method for MPPT in PV systems under partial shading conditions. *Renewable Energy*, 75, 308–317. <https://doi.org/10.1016/j.renene.2014.09.044>
- Taibi, D., Amieur, T., Laamayad, T., & Sedraoui, M. (2023). Improvement of the Standard Perturb & Observe MPPT control strategy by the proposed Fuzzy Logic Mechanism for a Cascade Regulation of a PMSM-based PV pumping system. *Arabian Journal for Science and Engineering*, 48(5), 6631–6647. <https://doi.org/10.1007/s13369-022-07496-9>
- Vitorino, M. A., De Rossiter Corrèa, M. B., Jacobina, C. B., & Lima, A. M. N. (2011). An effective induction motor control for photovoltaic pumping. *IEEE Transactions on Industrial Electronics*, 58(4), 1162–1170. <https://doi.org/10.1109/TIE.2010.2054053>
- Yang, B., Zhu, T., Wang, J., Shu, H., Yu, T., Zhang, X., Yao, W., & Sun, L. (2020). Comprehensive overview of maximum power point tracking algorithms of PV systems under partial shading condition. *Journal of Cleaner Production*, 268, 121983. <https://doi.org/10.1016/j.jclepro.2020.121983>
- Yap, K. Y., Sarimuthu, C. R., & Lim, J. M. Y. (2020). Artificial Intelligence Based MPPT Techniques for Solar Power System: A review. *Journal of Modern Power Systems and Clean Energy*, 8(6), 1043–1059. <https://doi.org/10.35833/MPCE.2020.000159>



© 2024. The Author(s). This article is an open access article distributed under the terms and conditions of the Creative Commons Attribution-ShareAlike 4.0 (CC BY-SA) International License (<http://creativecommons.org/licenses/by-sa/4.0/>)